Caenorhabditis elegans pathways that surveil and defend mitochondria

Published in final edited form as:
Nature. 2014 April 17; 508(7496): 406–410. doi:10.1038/nature13204.

Caenorhabditis elegans pathways that surveil and defend mitochondria

Ying Liu[1,2,3], **Buck S. Samuel**[1,2], **Peter C. Breen**[1,2], and **Gary Ruvkun**[1,2,*]

[1]Department of Molecular Biology, Massachusetts General Hospital, Boston, MA 02114, USA

[2]Department of Genetics, Harvard Medical School, Boston, MA 02115, USA

Abstract

Mitochondrial function is challenged by toxic byproducts of metabolism as well as by pathogen attack[1],[2]. *Caenorhabditis elegans* normally responds to mitochondrial dysfunction with activation of mitochondrial repair, drug detoxification, and pathogen-response pathways[1–7]. From a genome-wide RNAi screen, we identified 45 *C. elegans* genes that are required to upregulate detoxification, pathogen-response, and mitochondrial repair pathways after inhibition of mitochondrial function by drugs or genetic disruption. Animals defective in ceramide biosynthesis are deficient in mitochondrial surveillance, and addition of particular ceramides can rescue the surveillance defects. Ceramide can also rescue the mitochondrial surveillance defects of other gene inactivations, mapping these gene activities upstream of ceramide. Inhibition of the mevalonate pathway, either by RNAi or statin drugs also disrupts mitochondrial surveillance. Growth of *C. elegans* with a significant fraction of bacterial species from their natural habitat causes mitochondrial dysfunction. Other bacterial species inhibit *C. elegans* defense responses to a mitochondrial toxin, revealing bacterial countermeasures to animal defense.

Mitochondria are almost entirely composed of proteins encoded by the nuclear genome[8]. A surveillance pathway detects mitochondrial defects to induce mitochondrial chaperone genes *hsp-6* and *hsp-60* and xenobiotic detoxification and pathogen-response pathways[1–7]. Disrupting *C. elegans* mitochondrial function induces drug detoxification genes such as *cyp-14A3* and *ugt-61* (Figure 1a-c), as well as a *Pseudomonas* pathogen-response gene *irg-1*[9] (Figure 1d). This suggests that animals interpret a disruption of mitochondrial activity as a xenobiotic or pathogen attack. Consistent with this, *C. elegans* exhibits bacterial avoidance behavior when mitochondria are inhibited by RNAi or antimycin, an inhibitor of mitochondrial electron transport produced by *Streptomyces*[1] (Figure 1e and 1f). Animals also show aversive behaviors in the absence of any drug or mitochondrial gene inactivation

*Corresponding author: ruvkun@molbio.mgh.harvard.edu.
[3]Present address: State Key Laboratory of Biomembrane and Membrane Biotechnology, Institute of Molecular Medicine, Peking-Tsinghua Center for Life Sciences, Peking University, Beijing 100871, China

Author Contributions Y.L. and G.R. designed experiments; Y.L., B.S.S. and P.C.B. carried out experiments. Y.L., B.S.S. and G.R. wrote the paper. G.R. supervised the project.

if they carry a mutation of the nuclearly-encoded mitochondrial gene *isp-1(qm150)* (Figure 1g). This mutation also activates *hsp-6* (Figure 1h).

C. elegans live in microbe-rich environment[10]. We isolated microbes from habitats with wild *C. elegans* populations[10], classified them based on their 16S ribosomal sequences (Samuel BS, Félix MA and Ruvkun G, unpublished), and found that 18% of the 560 strains tested caused mitochondrial stress as revealed by induction of *hsp-6p::gfp* (Figure 2a-c). This suggests that mitochondria are targeted by many bacterial species, and explains the evolution of coupling detection of *C. elegans* mitochondrial dysfunction to antibacterial gene expression and behavioral responses. Iron is a valuable resource to microbes which often produce siderophores to capture the iron; the eukaryotic mitochondrion, rich in heme and iron sulfur proteins, is an attractive iron depot for bacteria. Bacterial toxins, siderophores or virulence factors from these many bacterial strains may target the mitochondrion.

To identify the molecular elements of how animal mitochondrial dysfunction is detected and coupled to a detoxification response, we performed a genome-wide RNAi screen for gene inactivations that render *C. elegans* unresponsive to mitochondrial dysfunction (Extended Data Figure 1 and 2). Gene inactivations that caused a failure to induce *hsp-6p::gfp* in antimycin were re-screened for failure to upregulate other genes normally induced by mitochondrial dysfunction: the detoxification gene *ugt-61::gfp* in antimycin, *hsp-6p::gfp* induction in the *isp-1(qm150)*, or *hsp-6p::gfp* induction by ATP synthase *atp-2* RNAi. Mitochondrial surveillance and response was disrupted by 45 gene inactivations (Extended Data Table 1), including the known components *atfs-1*, *clpp-1* and *dve-1* [4,6].

One of the gene inactivations that potently disrupts response to mitochondrial dysfunction, *sptl-1,* encodes serine palmitoyl transferase, in the sphingolipid biosynthesis pathway (Extended Data Figure 3). Inactivation of *sptl-1* by RNAi inhibited the induction of *hsp-6p::gfp* upon antimycin treatment or *spg-7*(RNAi) (Figure 3a and 3b), whereas *sptl-1*(RNAi) alone without antimycin treatment did not induce the expression of *hsp-6p::gfp* (Extended Data Figure 4b). *sptl-1*(RNAi) did not affect the activation of ER stress reporter *hsp-4p::gfp* by the drug tunicamycin (Figure 3c), indicating a specific role in mitochondrial surveillance. A probable null mutation in *sptl*-1 (Extended Data Figure 5a) impaired the induction of *hsp-6*, *cyp-14A3,* and *ugt-61* after mitochondrial disruption by *spg-7*(RNAi) (Figure 3d). A double mutant in the two ceramide synthase genes of the sphingolipid biosynthetic pathway also attenuated the induction of *hsp-6* upon mitochondrial damage (Extended Data Figure 5b). Treatment with myriocin, a fungal inhibitor of mammalian serine palmitoyl transferase, disrupted antimycin-induced *hsp-6p::gfp* induction (Figure 3e). *sptl-1*(RNAi) (with normal movement, Supplementary Video S1 and S2) attenuated food avoidance induced by antimycin or *spg-7*(RNAi), suggesting that this behavioral response is also coupled to *sptl-1* (Figure 3g, Extended Data Figure 4d and 4e). *sptl-1* expression is up-regulated 2.5-fold by mitochondrial damage (Extended Data Figure 4a), suggesting that increased sphingolipids during mitochondrial disruption may act as a signal rather than as a membrane component required for another signal.

The morphology of the normally extensive mitochondrial network of *C. elegans* and other animals is responsive to mutation or inactivation of mitochondrial components[11]. Mitochondria in *sptl-1*(RNAi) animals hyperfused into larger, longer mitochondria (Figure 3f), suggesting that *sptl-1* is critical for mitochondrial homeostasis. The *isp-1* mitochondrial mutant had a severe synthetic growth defect on *sptl-1*(RNAi), whereas wild type development was only slightly delayed on *sptl-1*(RNAi) (Figure 3h). Sphingolipid signaling may act in the homeostatic response to the mitochondrial defect caused by the *isp-1(qm150)* mutation; in the absence of that response, *isp-1(qm150)* may cause a more severe mitochondrial defect and growth arrest. *sptl-1*(RNAi) animals were also more sensitive to the mitochondrial inhibitor antimycin (Extended Data Figure 4f). Additionally, *sptl-1*(RNAi) animals were unable to sense mitochondrial inhibition and activate the mitochondrial surveillance pathway when challenged by a set of the wild microbes that disrupt mitochondrial function (Extended Data Figure 4g).

Ceramide supplementation rescued the *sptl-1* defect in mitochondrial surveillance (Figure 4a and Extended Data Figure 5d), whereas ceramide in the absence of mitochondrial damage did not induce *hsp-6p::gfp* (Extended Data Figure 5e), suggesting that ceramide is not a sufficient signal to induce the suite of responses to mitochondrial dysfunction in the absence of true mitochondrial dysfunction. Ceramide supplementation also partially rescued the mitochondrial morphology defect (Figure 4b) and the impaired food avoidance behavior caused by *sptl-1*(RNAi) (Extended Data Figure 6a). Dihydroceramide, a ceramide precursor with no signaling function in mammals, could not rescue the *sptl-1*(RNAi) mitochondrial surveillance defect (Figure 4a). Two *C. elegans* ceramide synthases HYL-1 and HYL-2 synthesize different ceramide species, C24 to C26, and C20 to C22 ceramides, respectively[12]. Testing C16, C20, C22 and C24 ceramides, only C24 ceramide rescued the deficiency of mitochondrial surveillance caused by *sptl-1*(RNAi) (Figure 4c).

During apoptosis and mitophagy, ceramide accumulates on the outer membrane of mitochondria[13–15]. Using antibodies to stain ceramide and the mitochondrial protein oxidative phosphorylation Complex IV (COX-IV), ceramide and mitochondrial protein colocalization dramatically increased after *C. elegans* mitochondrial inhibition (Figure 4d). The increased colocalization preceded induction of *hsp-6p::gfp* (Extended Data Figure 6b and 6c). Thus, ceramide may participate in an early step of mitochondrial surveillance by marking domains of dysfunction.

To map ceramide relative to other gene inactivations that render animals unable to respond to mitochondrial damage, we tested if ceramide could rescue the mitochondrial surveillance defects of other hits from the RNAi screen. Five other gene inactivations were rescued by ceramide: *ran-4*, a nuclear transport component*; Y47G6A.29,* a phosphatidyl inositol signaling component*; F40F12.7*, a zinc finger protein*; Y54E10BR.5*, a signal peptidase component; *and ceh-20*, a homeobox transcription factor (Extended Data Figure 6e). These gene inactivations may disrupt mitochondrial surveillance upstream of the production of ceramide.

ATFS-1 is a transcription factor that activates *hsp-6* and *hsp-60* during mitochondrial stress (Figure 4e)[5]. ATFS-1 contains an N-terminal mitochondrial targeting sequence as well as a

nuclear localization signal; when mitochondria are damaged, nuclear accumulation of ATFS-1 is favored[6]. Deletion of the N-terminal 1–32 amino acid causes constitutive nuclear accumulation of ATFS-1 (Extended Data Figure 6d) and activates *hsp-60p::gfp*[6]. Activation of *hsp-60p::gfp* by ATFS-1$^{\Delta 1-32.myc}$ did not require *sptl-1* gene activity (Figure 4f), suggesting that ceramide works upstream of ATFS-1 and plays a role in the early detection of mitochondrial dysfunction.

hmgs-1 which encodes HMG-CoA (3-hydroxy-3-methyl-glutaryl-CoA) synthase of the mevalonate synthetic pathway is also a strong hit from the genome-wide screen. *hmgs-1* gene inactivation inhibited antimycin-induced *hsp-6p::gfp* induction and food avoidance (Extended Data Figure 7a-d). *hmgs-1*(RNAi) also induced abnormal mitochondrial morphology (Extended Data Figure 7e). Supplementing mevalonate to *hmgs-1*(RNAi) animals rescued the deficiency of antimycin-induced *hsp-6p::gfp* (Extended Data Figure 7f).

Statins are cholesterol-lowering drugs that inhibit the mevalonate pathway (Extended Data Figure 8a)[16]. Treating *C. elegans* with statins also abrogates their ability to sense mitochondrial damage and activate protective programs (Extended Data Figure 7g and 8b). A common side effect of statin therapy is muscle toxicity[17]. By inhibiting the mevalonate pathway, statins inhibit ubiquinone synthesis, a key component of the electron transport chain (Extended Data Figure 8a). Our data suggests that a combined inhibition of ubiquinone synthesis and mitochondrial surveillance may contribute to the muscle toxicity of statins. In support of a role for mitochondrial surveillance in statin action, a gain-of-function mutation in *C. elegans atfs-1* confers statin resistance[18]. Treating human embryonic kidney HEK293T cells with statin impaired the mitochondrial network and morphology (Extended Data Figure 7h and 9). Statin treatment also decreased ATP production in mouse C2C12 myotubes (Extended Data Figure 7i).

Eukaryotic mitochondrial surveillance pathway components are likely to be targets of microbial toxins and virulence factors. If the animal surveillance of the mitochondria is disabled by a bacterial toxin or virulence factor, other anti-mitochondrial toxins, siderophores, or virulence factors would be rendered more effective. To detect such bacterial anti-surveillance activities, we screened our collection of *C. elegans* flora for bacterial species which when co-cultured with *C. elegans* could disrupt the induction of *hsp-6p::gfp* by antimycin. Six wild bacterial strains of the genus *Pseudomonas* from three species (*vranovensis*, *brenneri* and *asplenii*) disrupt mitochondrial surveillance (Figure 2d and 2e). The dozens of *C. elegans* genes we have identified in the mitochondrial surveillance pathway are candidate targets for toxins or virulence factors from these *Pseudomonas* strains.

Our studies have revealed roles of ceramide and mevalonate in mitochondrial surveillance. The products of these pathways either constitute signals that are transferred within or between cells, or structures within those cells that are necessary for other signals to emerge. We favor that these constitute signals because the expression of these biosynthetic pathways are induced by the mitochondrial insults (Extended Data Figure 4a) and because these molecules are localized to the site of injury (Figure 4d). Ceramides are upstream elements of the stress response of plasma membrane, ER and mitochondria in multiple species[19,20], and

can act as hormonal signals[21]. But it is also possible that these constitute membrane elements required for other signals. Variation in the animal pathways for mitochondrial surveillance that we have identified, many of which encode conserved proteins, may underlie variation in the symptoms causes by the same mitochondrial mutations or variation in response to mitochondrial toxins such as the statins. Microbial secondary metabolites that render animals unresponsive to their mitochondrial dysfunctions (Figure 2d and 2e), may have therapeutic potential in the treatment of a predicted up-regulation of detoxification and anti-bacterial pathways which may contribute to the devastating symptoms of some mitochondrial diseases. The anti-surveillance activities of such natural products may also treat other disorders of dysregulated detoxification and innate immunity, such as autoimmunity.

Methods

C. elegans strains

hsp-6p::gfp(zcIs13)V, *dpy-5(e907)I; ugt-61p::gfp(sEX11571)*, *hsp-4p::gfp (zcIs4)V*, *myo-3p::GFPmt(zcIs14), isp-1(qm150)*, *sptl-1(ok1693)II*, *tag-38(ok490)V*, *lagr-1(gk327) I; hyl-1(ok976) IV*, *sphk-1(ok1097) II*, *hyl-2(ok1766) X*, *hyl-2(gnv1) X*, and *asm-3(ok1744) IV* were obtained from the Caenorhabditis Genetics Center (CGC). *irg-1p::gfp* was provided by Fred Ausubel. *isp-1; hsp-6p::gfp* was generated by crossing *hsp-6p::gfp* into *isp-1(qm150)*. *atfs-1; hsp-60p::gfp, atfs-1(tm4525); hsp-16p::atfs-1*$^{\Delta 1\text{-}32.myc}$*::gfp* and *atfs-1(tm4525)*; *hsp-16p::*ATFS-1$^{\Delta 1\text{-}32.myc}$; *hsp-60p::gfp* were provided by Cole Haynes. Hermaphrodites were used throughout of the study.

Activation of GFP reporter by wild microbes

Wild microbes isolated from various habitats harboring wild *C. elegans* populations[10] (Samuel BS, Félix MA and Ruvkun G, unpublished) were grown in LB at 18°C shaking for 16–18hrs, concentrated 3X and seeded (30ul) into 24-well NGM plates (no antibiotics) in duplicate. Plates were dried and allowed to grow overnight at room temperature before ~40 synchronized L1 worms were added to the wells. Animals were scored after 48hrs at 20°C. Genera with more than 3 independent isolates that induced *hsp-6p::gfp* expression are noted along with the percentage of total microbes tested (Figure 2a). Other genera that strongly activate *hsp-6p::gfp* expression, include *Achromobacter*, *Curtobacterium*, *Enterobacter*, *Leucobacter*, *Mycetocola*, *Myroides*, *Raoultella* and *Rhodococcus*.

Activation of GFP reporter by RNAi

RNAi clones were grown in LB containing 50ug/ml carbenicillin at 37 °C overnight and seeded 100ul/well to 24-well worm plates with 5mM IPTG. Dried plates were kept at room temperature overnight to allow IPTG induction of dsRNA expression. Synchronized L1 worms (~40 worms/well) were raised on the RNAi plate at 20 °C. Fluorescence was assayed at 48 hours.

Activation of GFP reporter by drugs

Synchronized L1 worms (~40 worms/well) were raised on a 24-well plate at 20 °C for 48 hours. At this time, each well was treated with 0.5ug antimycin (total volume 20ul) in M9

buffer (3g KH_2PO_4, 6g Na_2HPO_4, 5g NaCl, 1ml 1M $MgSO_4$, H_2O to 1L), or 1.5ug tunicamycin in DMSO (total volume 20ul). GFP expression was assayed after 24 hours (antimycin), or 7 hours (tunicamycin).

Microscopy

Comparable GFP reporter images were obtained by a Zeiss AxioImager Z1 using the same exposure time. Mitochondrial morphology of *C. elegans* or HEK293T cells was visualized under an Olympus Fluoview 1000 confocal microscope.

Genome-wide RNAi screen

Primary screen was performed by seeding individual bacterial clones each bearing a distinct *C. elegans* dsRNA to initiate RNAi onto 24-well RNAi plates. Dried plates were kept at room temperature overnight to induce the expression of dsRNAs. Synchronized L1 *hsp-6p::gfp* worms (~40 animals/well) were raised on the 24-well plate at 20 °C for 48 hours. At this time, each well was treated with 0.5ug antimycin in M9 buffer (total volume 20ul). GFP expression was assayed after 24 hours. Scores were recorded from 0 (no inhibition of GFP expression) to 4 (strong inhibition of GFP expression).

Positive clones from the primary screen were picked and re-screened in multiple parallel secondary screens. For one screen, synchronized L1 *hsp-6p::gfp* worms (~40 animals/well) were raised on 24-well plate at 20 °C for 36 hours. At this time, each well was treated with 20-fold concentrated *E. coli* expressing *atp-2* dsRNA (total volume 20ul), to inactivate the mitochondria using RNAi rather than using the antimycin of the primary screen. GFP expression was assayed after 36 hours. In a third test, synchronized L1 *isp-1(qm150); hsp-6p::gfp* (2 animals/well) were dropped onto 24-well plate using a worm sorter, and raised at 20 °C. This strain carries a mitochondrial mutation that activates *hsp-6p::gfp* expression in untreated animals as well as in most wells. Fluorescence were scored when they reached L4 stage and again when their progeny (if the strains were fertile) developed to the L4 stage. In a fourth parallel screen, synchronized L1 *ugt-61p::gfp* worms (~40 animals/well) were raised on 24-well plate at 20 °C for 48 hours. At this time, each well was treated with 0.5ug antimycin in M9 (total volume 20ul). GFP expression was assayed after 24 hours.

Western blotting

Synchronized worms were raised on plates under described conditions. Worms were then washed off plates, resuspended with NuPAGE® LDS Sample Buffer (Invitrogen) and boiled at 95°C for 5 min. Lysates containing the same amount of protein were loaded onto SDS-PAGE and transferred onto Nitrocellulose membrane (Invitrogen). After blocked with 5% nonfat milk, the membrane was probed with the designated first and second antibodies and developed with the enhanced chemiluminescence method (Perkin Elmer) and visualized by X-ray film.

RNA isolation and quantitative RT- PCR

Synchronized L1 wild-type N2 and mutant worms were raised on control or *spg-7*(RNAi) at 20 °C, and harvested at the L4 stage. Worms were then washed, resuspended with Trizol

reagent (Invitrogen), frozen and homogenized by grinding. Total RNA was isolated by chloroform extraction, followed by ethanol precipitation and DNase treatment (Ambion, Turbo DNA free kit). cDNA was then synthesized by reverse transcription (Invitrogen, SuperScript® III First-Strand Synthesis System). Quantitative real-time PCR was carried out using SYBR GREEN PCR Master Mix (Bio-Rad). Quantification of transcripts was normalized to *rpl-32* and relative expression levels were calculated as previously described[22].

Food avoidance assays

Each gene inactivation that disrupted the response to mitochondrial dysfunction was grown in 1ml LB containing 50ug/ml carbenicillin at 37 °C overnight, pelleted, resuspended with 50ul LB and dropped in the center of a well of 6-well plates containing 5mM IPTG. Dried plates were kept at room temperature overnight to allow IPTG induction of dsRNA expression. Only circular lawns of uniform size and density were used for food avoidance assays. Synchronized L1 worms (~100 animals/well) were dropped in the center of each bacterial lawn. Food avoidance phenotypes were scored at 48 hours. For antimycin treatment, synchronized L1 worms (~100 animals/well) were dropped in the center of each bacterial lawn, and grown at 20 °C for 48 hours. At this time, 50ug antimycin (total volume 80ul) was added directly to the bacteria lawn. Food avoidance was score 8 hours after drug treatment.

Synthetic growth defect on *sptl-1*(RNAi)

Wild type N2 or mitochondrial mutant allele *isp-1* animals were synchronized at the L1 stage. Animals were then raised on control or *sptl-1*(RNAi). *isp-1* animals were grown on control RNAi for 3 days vs. on *sptl-1*(RNAi) for 5 days to match the developmental stage of wild type N2 animals.

Ceramide biosynthetic mutant analyses

To dissect the pathway of *sptl-1* function in mitochondrial surveillance, we tested other mutations in the sphingolipid biosynthetic pathway (Extended Data Figure 4 and 5a). Inactivation of another serine palmitoyl transferase gene *sptl-3* had no effect on the induction of *hsp-6* upon mitochondrial damage (Extended Data Figure 4, 5a and 5b). A double mutation of *hyl-1* and *lagr-1*, which encode ceramide synthases, reduced the induction of *hsp-6* upon mitochondrial damage (Extended Data Figure 5b), whereas *hyl-1* or *lagr-1* single mutants were less defective (Extended Data Figure 5c). Only the C24 ceramide, synthesized by HYL-1, rescued the deficiency of mitochondrial surveillance caused by *sptl-1*(RNAi). This is consistent with the defect in *hsp-6* induction shown in the *hyl-1; lagr-1* double mutant (Extended Data Figure 5b).

Immunostaining

Immunostaining of dissected animals was carried out according to Philips et al[23] with minor modifications. Specifically, dissected animals were blocked with 0.5% BSA in PBST for 1 hour at room temperature, and stained with anti-ceramide antibody [MID15B4, Alexis Biochemicals diluted 1:60 (v/v)] in 0.2% BSA in PBST and anti-human OxPhos Complex

IV antibody [Invitrogen diluted 1:30 (v/v)] at room temperature for half hour and 4°C overnight. Followed three washes with PBST (10 min each time), slides were then incubated with Cy-3 anti-mouse secondary antibody [diluted 1:200 (v/v)] for 1 hour at room temperature. After three washes again with PBST (10 min each time), slides were mounted and visualized under an Olympus Fluoview 1000 confocal microscope.

HEK293T cells (ATCC) were washed twice with ice cold PBS and fixed with 4% formaldehyde at 4°C for 1 hour. After fixation, cells were permeabilized by 0.1% Triton in PBS at room temperature for 8 minutes, and then blocked with 0.5% BSA in PBST for 1 hour at room temperature, and stained with anti-human OxPhos Complex IV antibody [Invitrogen diluted 1:30 (v/v)] at room temperature for half hour and 4°C overnight. Following three washes with PBST (10 min each time), slides were mounted and visualized under an Olympus Fluoview 1000 confocal microscope.

ATP levels

C2C12 myoblasts (ATCC) were grown in Dulbecco's Modified Eagle Medium supplemented with 10% (v/v) fetal bovine serum and antibiotics (100 mg/mL penicillin/streptomycin mix) at 37 °C. Differentiation into myotubes was induced at ~90% density by changing the medium to DMEM supplemented with 2% (v/v) horse serum. Differentiation occurred after 5 days. Myotubes were then treated with DMSO, 10 μM simvastatin or 10uM mevastatin. After incubation for 48 h, CellTiter-Glo reagent (Promega) was added to cell-culture medium, and luminescence was measured after 10 min incubation.

Primers for quantitative RT-PCR

Detects	Forward primer, Reverse primer
hsp-6	CAAACTCCTGTGTCAGTATCATGGAAGG, GCTGGCTTTGACAATCTTGTATGGAACG
cyp-14A3	CAGTTTCCCGCCGAAAACATCCATTTG, CAATGCCGTTCTTCTTTGAAGCCTCCAG
ugt-61	GCAATTGGAGGTCATGACGTAACTATG, GCGAAGAATGATTCGGCATCCATCTTG
rpl-32	AGGGAATTGATAACCGTGTCCGCA, TGTAGGACTGCATGAGGAGCATGT
sptl-1	CTGAAAGGCAGAAAGATGAATTAATTGC, GAATCCACGTGGCCCGCACGATCCTACG

Primers for genotyping

gene name	Forward primer, Reverse primer
sptl-1	AGCCCAAGCCAATTATCCTT, AACACGAACTTTGAATCGCC
sptl-3	CTTGGTGTCCCTTTCGTGTT, AGGGCAAGAATTGGGGTAAT
F27E5.1	TGAAAGACAACTTGCTCGGA, TGTCTTTTCAGCAGTCACCG
T10B11.2	TCATTCCGACGGTACCATTT, TGAAGCTTGAAATGCAGTGG
asm-3	CTTGCACTCCTCCTTTCCAC, GGTGACAGAATGCGAGGAAT
hyl-1	GCCCCGTAAATAAGCACAAA, TCGTGTTCTTTCACGTCTCG
hyl-2	GGGGGAGTGATGGAAGAAAT, TTGCAAACCAATTGCAAGAA
lagr-1	ATGCTTGGACCTGAATAC, TTACACGTTCTTCGGTTTAAG

gene name	Forward primer, Reverse primer
sphk-1	ATGTTCATAGTAGTGGTAAC, CTAGGCAGTTGATGAGAAAACG

Extended Data

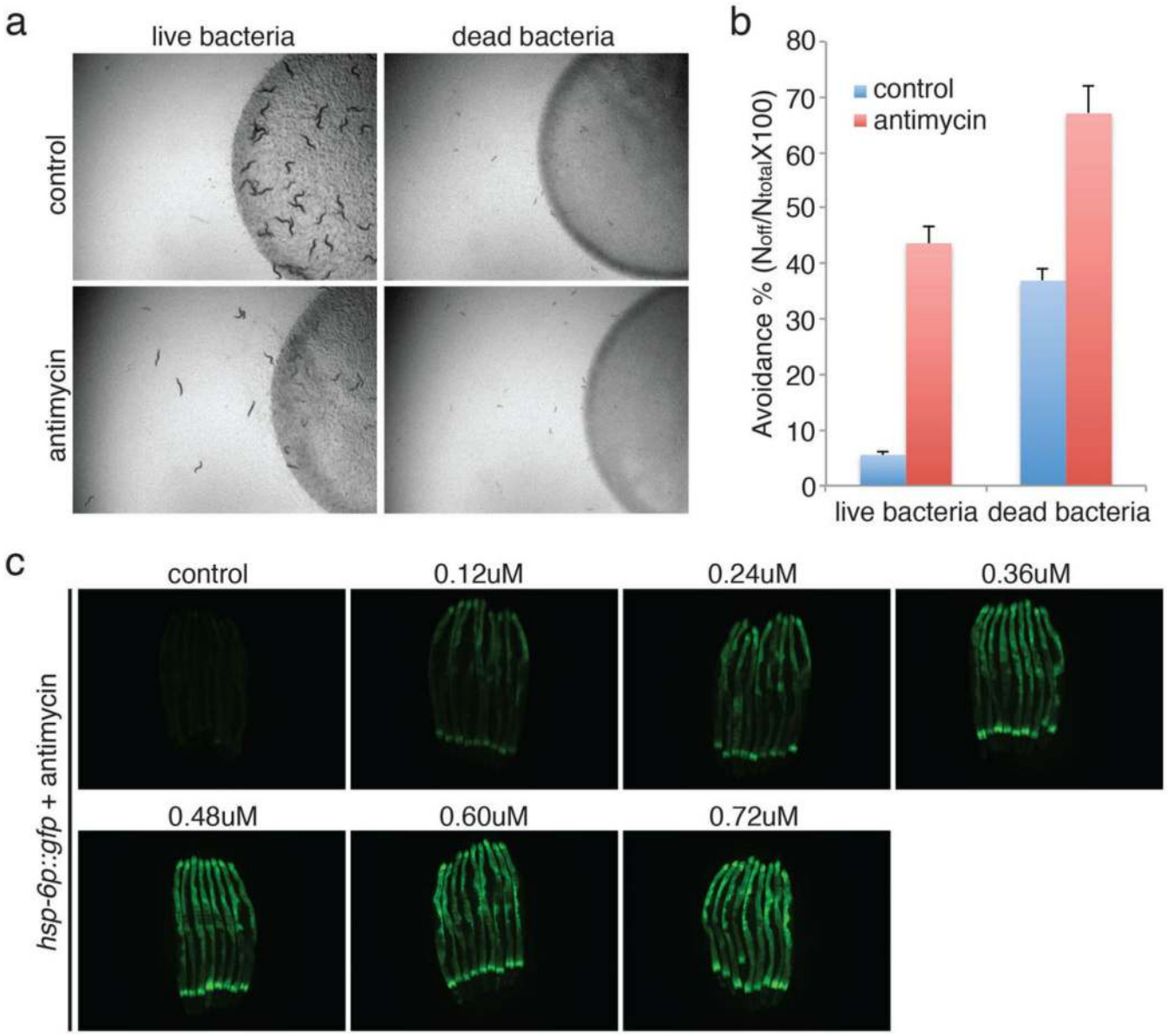

Extended Data Figure 1.

Mitochondrial dysfunction activates homeostatic, detoxification and pathogen responses. **a,** Drug-induced food avoidance phenotypes on live or dead bacteria. Dead bacteria were obtained by heating bacteria at 90 °C for 30 min. Avoidance behavior was also observed when antimycin was added to dead bacteria, showing that the drug acts directly on *C. elegans* and is not transformed by the bacteria. **b,** Quantification of the food avoidance

phenotypes of Extended Data Figure 1a (n=4). Error bars represent s.d. **c,** A dose response of *hsp-6p::gfp* induction with the addition of antimycin.

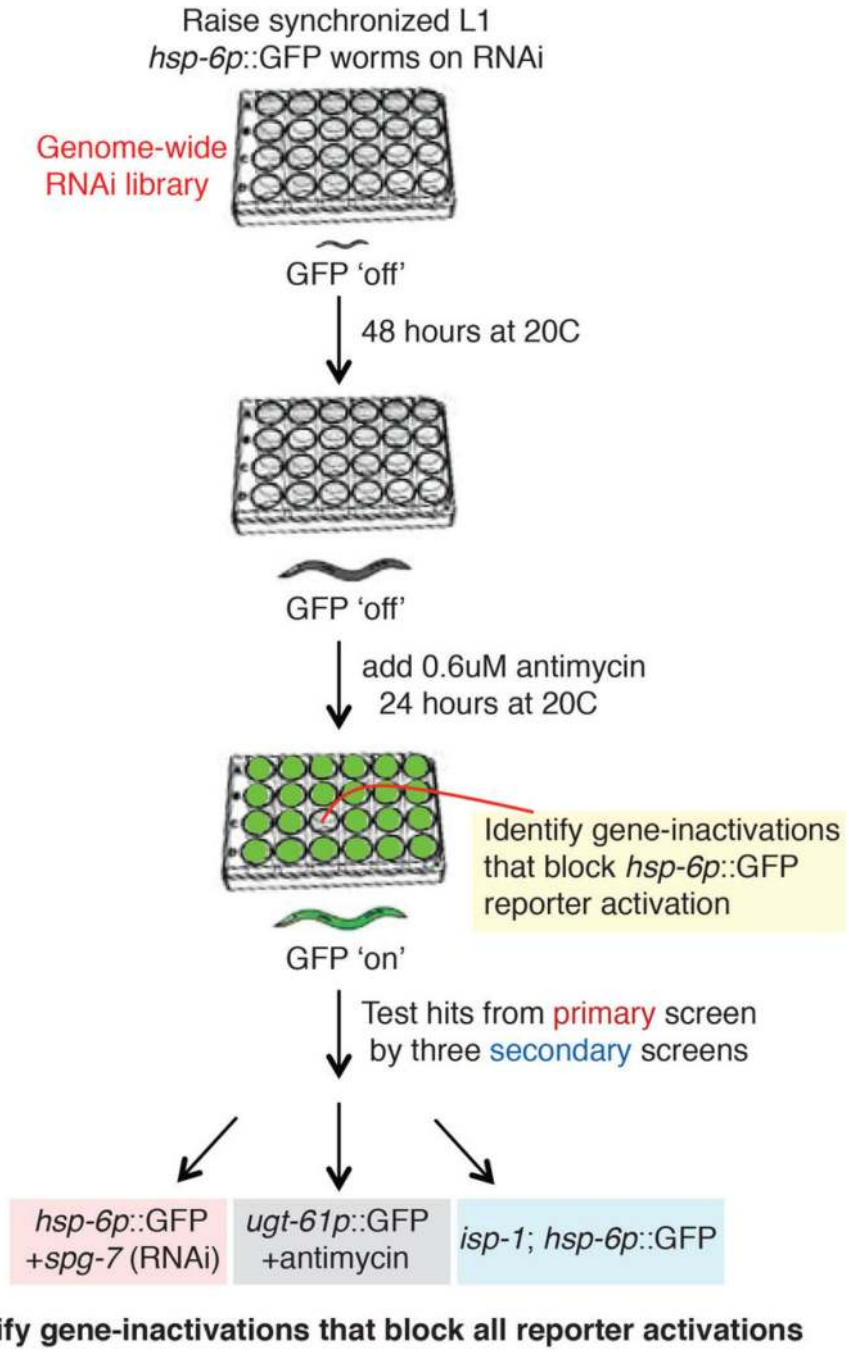

Extended Data Figure 2.

Diagram of the genome-wide RNAi screen workflow. For the detailed experimental procedure, see Methods.

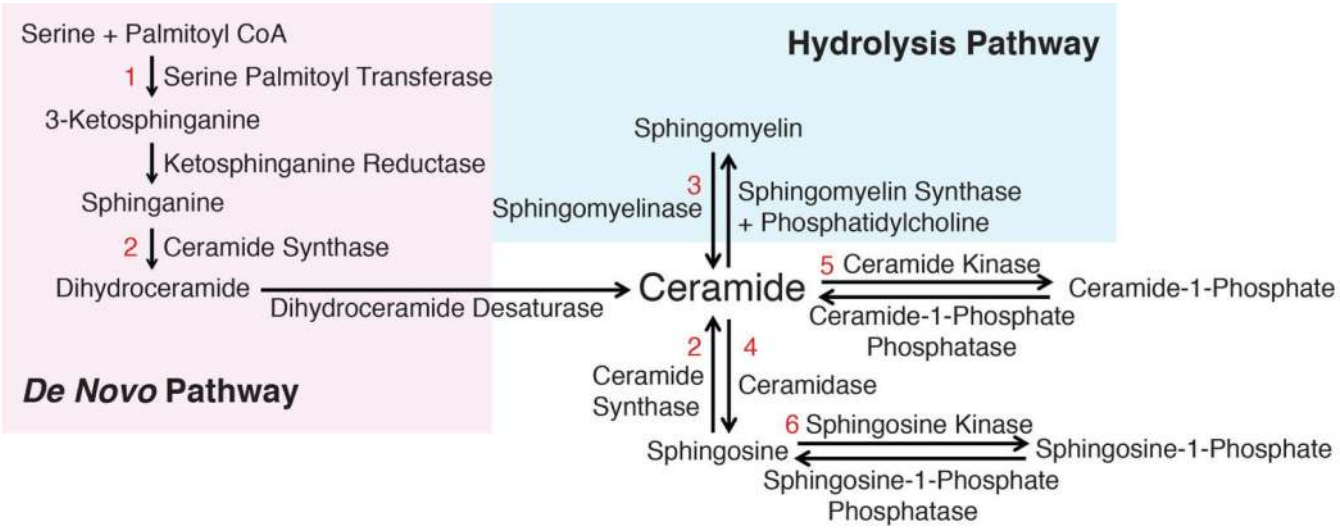

Gene product	Sequence name	*C. elegans* gene	Alleles
1. Serine Palmitoyl Transferase	C23H3.4	*sptl-1*	*ok1693*
	T22G5.5	*sptl-3*	*ok1927*
2. Ceramide Synthase	K02G10.6	*hyl-2*	*gnv1*
	C09G4.1	*hyl-1*	*ok976*
	Y6B3B.10	*lagr-1*	*gk327*
3. Sphingomyelinase	W03G1.7a,b	*asm-3*	*tm2384*
	T27F6.6		*tm2178*
4. Ceramidase	F27E5.1		*ok564*
5. Ceramide Kinase	T10B11.2		*ok1252*
6. Sphingosine Kinase	C34C6.5a,b	*sphk-1*	*ok1097*

Extended Data Figure 3.
Diagram of the sphingolipid metabolism pathway and the corresponding genes.

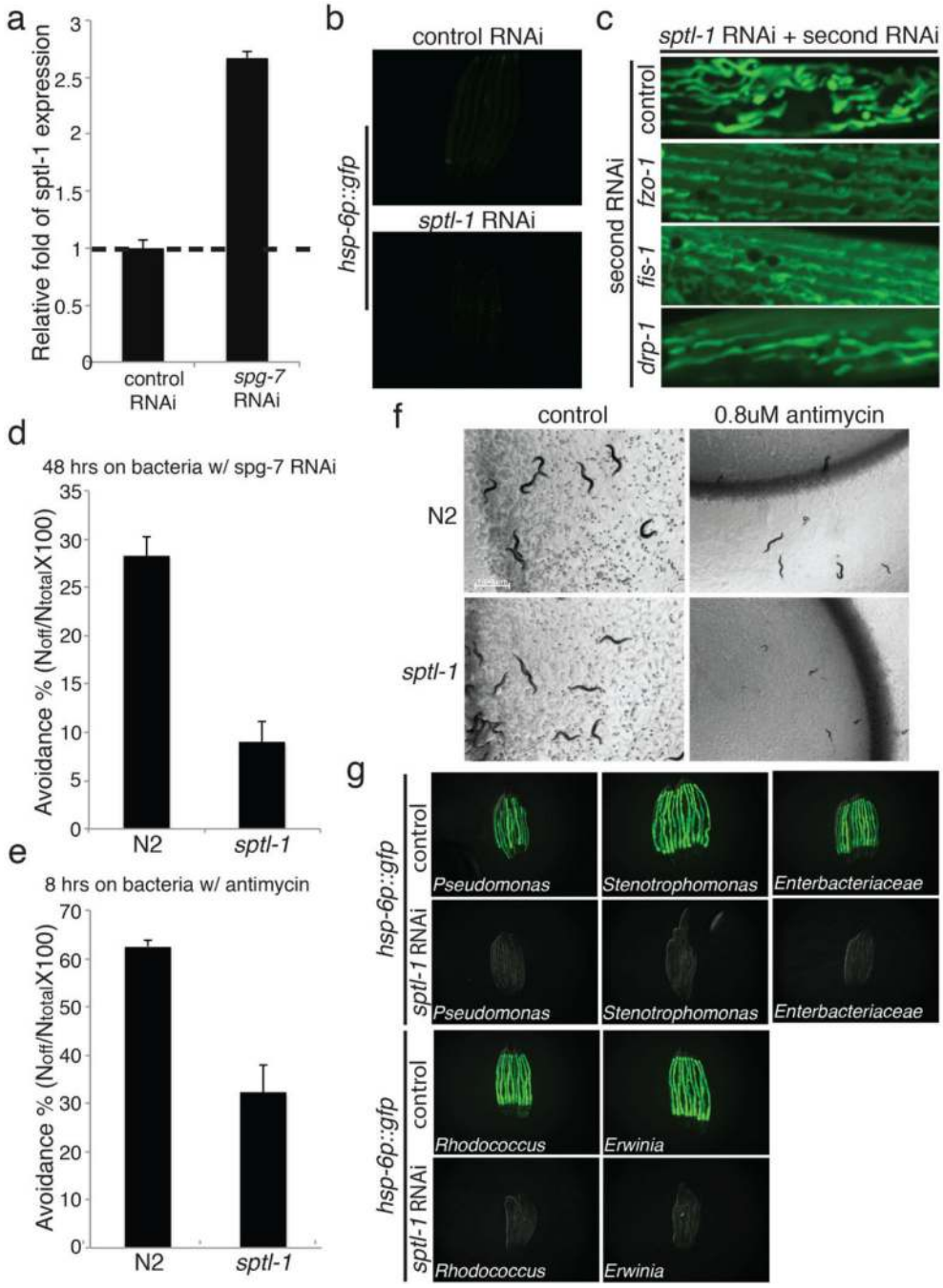

Extended Data Figure 4.

sptl-1 is required for mitochondrial surveillance. **a,** A graph showing the fold change in *C. elegans sptl-1* transcript level compared to control (n=3). Error bars represent s.d. **b,** *hsp-6p::gfp* worms raised on control or *sptl-1*(RNAi) (n=40). **c,** Body wall muscle animals expressing a mitochondrially localized GFP reporter. The animals were subjected to *sptl-1*(RNAi) for 36 hours and transferred onto the second RNAi (control, *fzo-1*, *fis-1* or *drp-1*). The hyperfusion of mitochondria observed under *sptl-1*(RNAi) is dependent on the fusion machinery as disruption of mitochondrial fusion by inactivating *fzo-1* or *fis-1*

partially restored the tubular structure. In contrast, inhibition of the gene *drp-1* that governs fission led to mitochondrial hyperfusion. The images were taken 36 hours after they were placed on the second RNAi. **d,** A graph showing the percentage of worms which avoid the *spg-7*(RNAi) bacteria lawn 48 hours after they were initially placed on the plates (n=4). Error bars represent s.d. **e,** A graph showing the percentage of worms which avoid the bacteria lawn 8 hours after the addition of antimycin (n=4). Error bars represent s.d. **f,** wild type N2 or *sptl-1(ok1693)* mutant animals raised in the presence or absence of 0.8μM antimycin. Photos were taken 4 days after the synchronized L1 worms were placed on the plates. **g,** *hsp-6p::gfp* animals were raised on *sptl-1*(RNAi) for 36 hours and transferred onto a subset of wild microbes. The images were taken after 2 days.

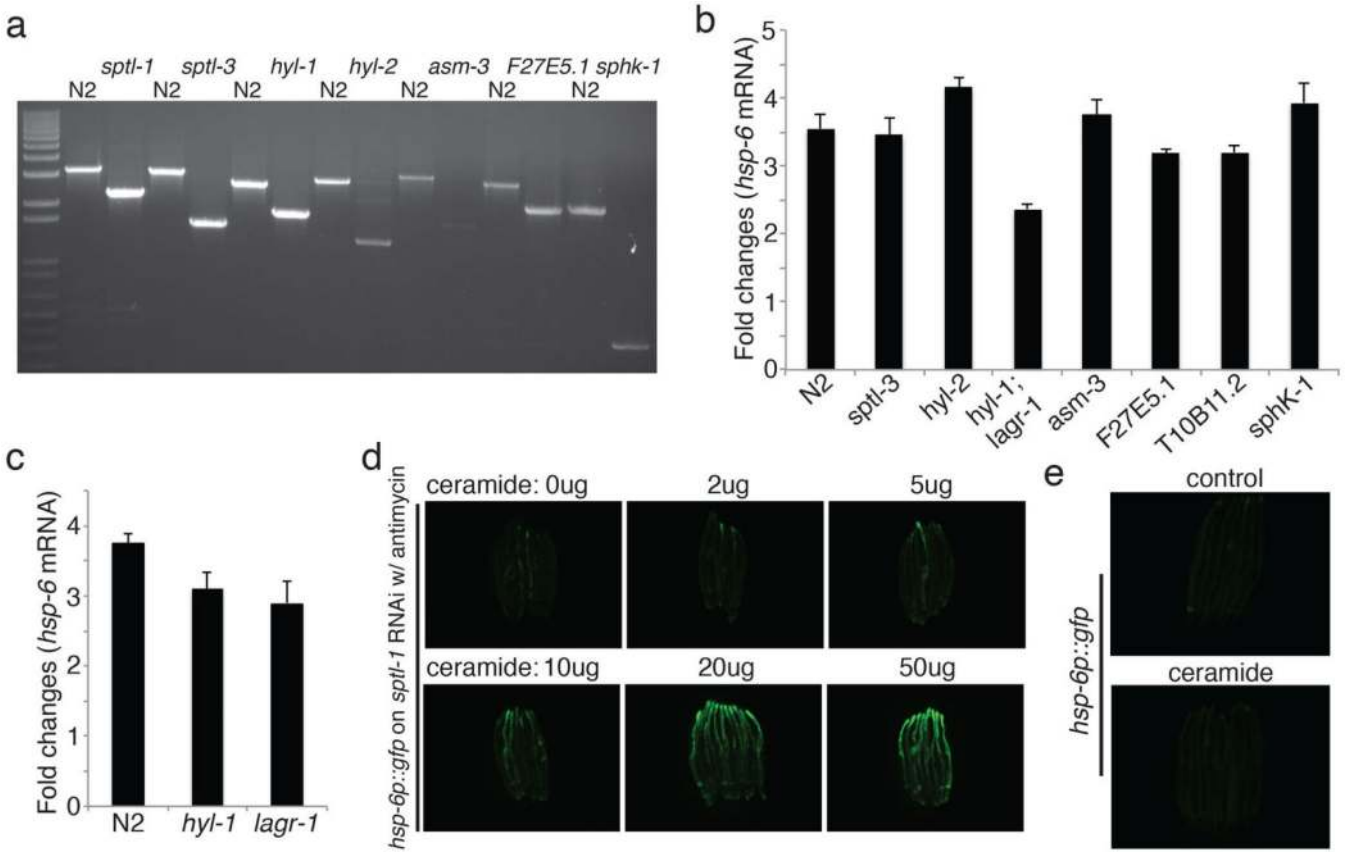

Extended Data Figure 5.

Ceramide biosynthesis is required for mitochondrial surveillance. **a,** Genotyping of the sphingolipid metabolism pathway mutant alleles. **b-c,** Fold difference in *hsp-6* transcript levels in wild type or sphingolipid metabolism pathway mutants (b) and *hyl-1* or *lagr-1* mutants (c) (n=3). Error bars represent s.d. **d,** *hsp-6p::gfp* worms raised on *sptl-1*(RNAi) in the presence of increasing amounts of ceramide. **e,** *hsp-6p::gfp* in the presence or absence of ceramide.

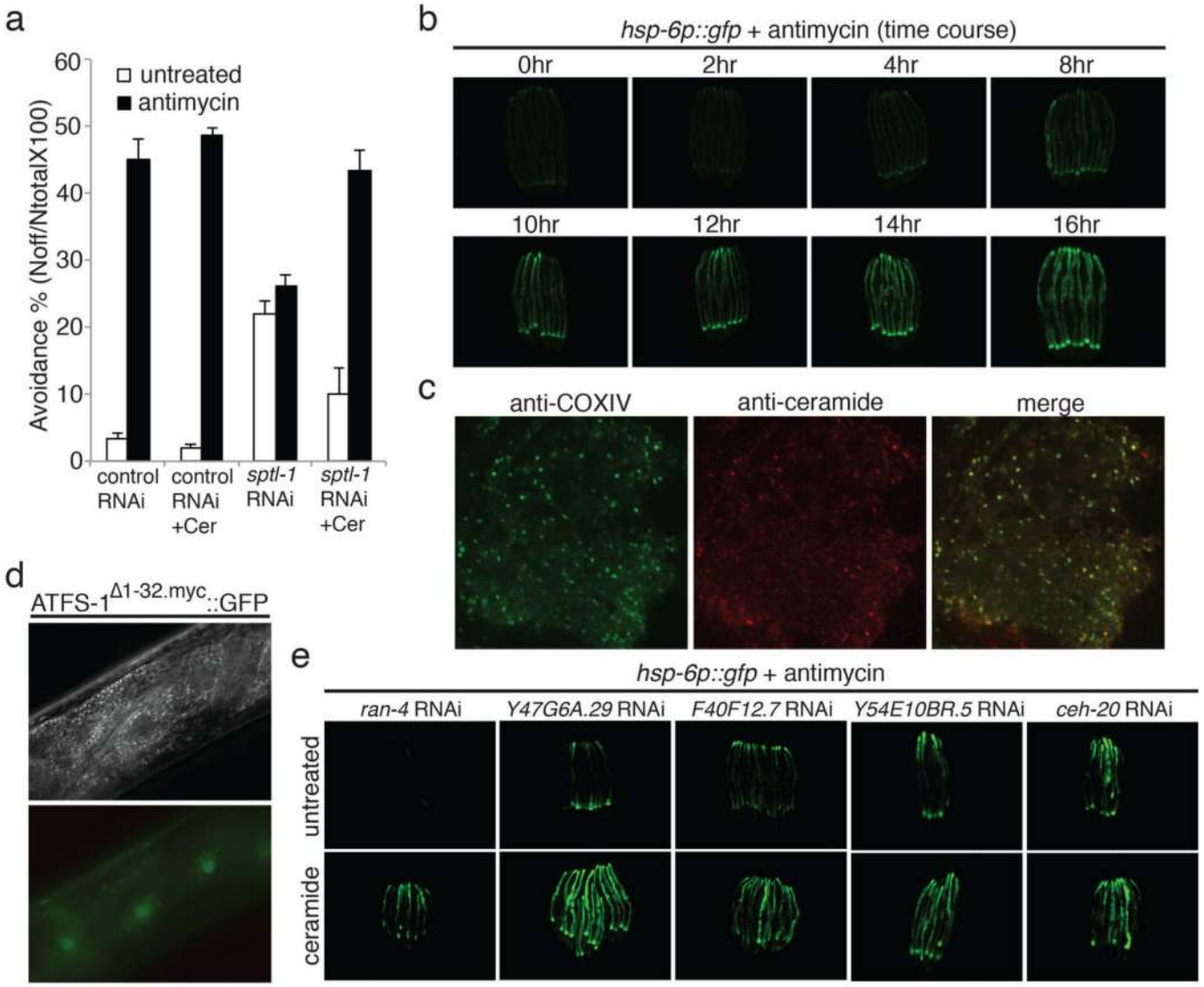

Extended Data Figure 6.

Ceramide biogenesis is required for mitochondrial surveillance. **a,** The percentage of worms that avoid the bacterial lawn 8 hours after the addition of antimycin. Animals were pre-treated with control RNAi, control RNAi with ceramide, *sptl-1* RNAi or *sptl-1* RNAi with ceramide (n=4). Error bars represent s.d. **b,** Time course experiment for the induction of *hsp-6p::gfp* with antimycin. **c,** Dissected young adults after 4 hours antimycin treatment were stained with anti-COX-IV antibody (red) and anti-ceramide antibody (green). **d,** Nomarski (upper panel) and fluorescent (lower panel) images of intestinal cells in *atfs-1; hsp-16p::atfs-1*$^{\Delta 1\text{-}32.myc}$*::gfp* transgenic animals. **e,** *hsp-6p::gfp* worms raised on indicated RNAi in the presence or absence of ceramide.

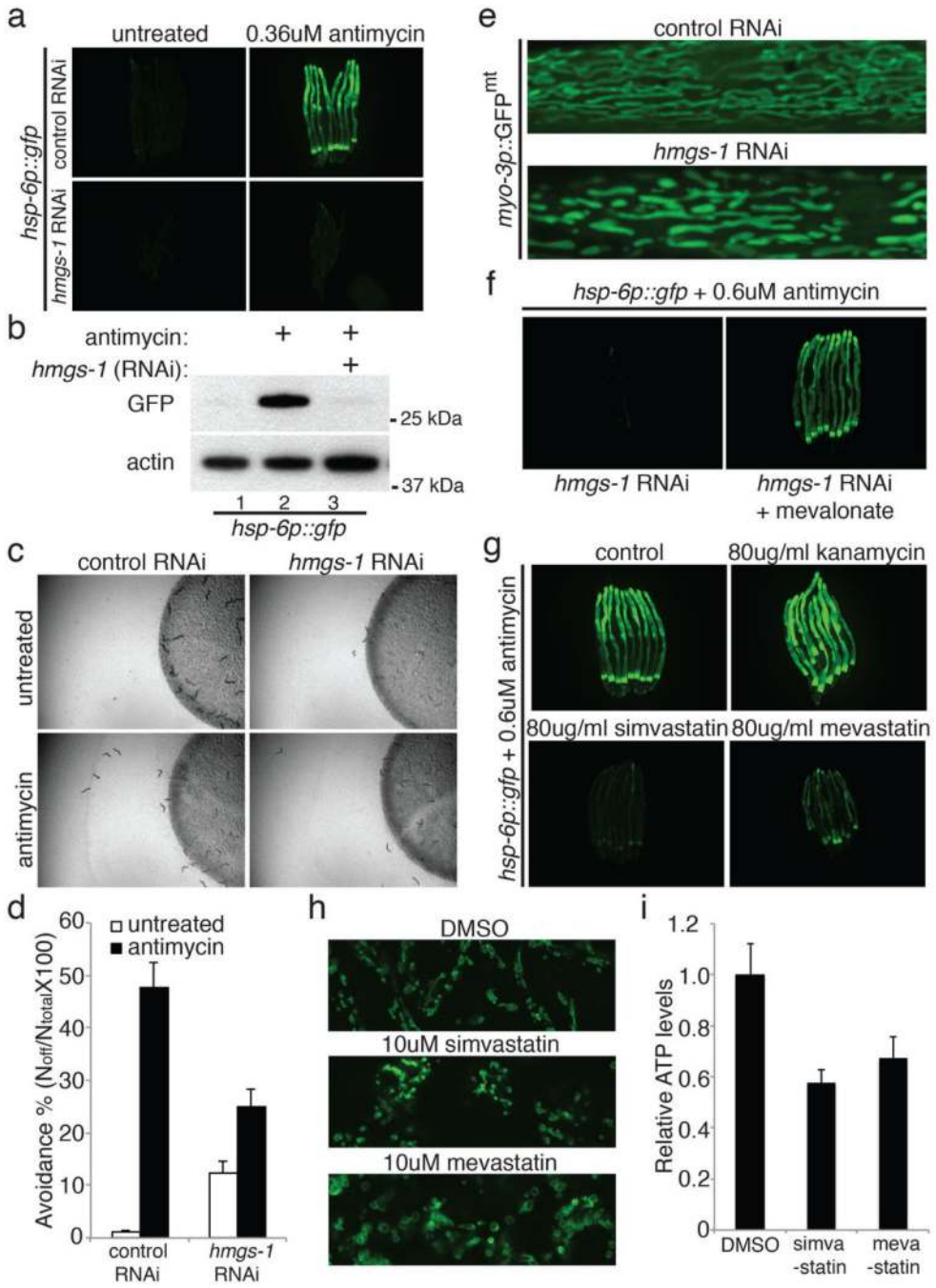

Extended Data Figure 7.

Inhibition of the mevalonate pathway disrupts mitochondrial surveillance. **a,** *hsp-6p::gfp* animals raised on control or *hmgs-1*(RNAi) in the presence of antimycin. **b,** Immunoblotting of GFP expressed by *hsp-6p::gfp* animals, with or without antimycin. **c,** Antimycin induced food avoidance in control or *hmgs-1*(RNAi) animals. **d,** Quantification of food avoidance (n=4). Error bars represent s.d. **e,** Body wall muscle of control or *hmgs-1*(RNAi) animals expressing a mitochondrially localized GFP reporter. **f,** *hsp-6p::gfp* animals raised on *hmgs-1*(RNAi), or *hmgs-1*(RNAi) with addition of mevalonate exposed to antimycin. **g,**

hsp-6p::gfp animals treated with antimycin after pre-treatment with simvastatin or mevastatin. **h,** Mitochondrial immunostaining in HEK293T cells. **i,** ATP levels in C2C12 myotubes after treating with simvastatin or mevastatin (n=3). Error bars represent s.d.

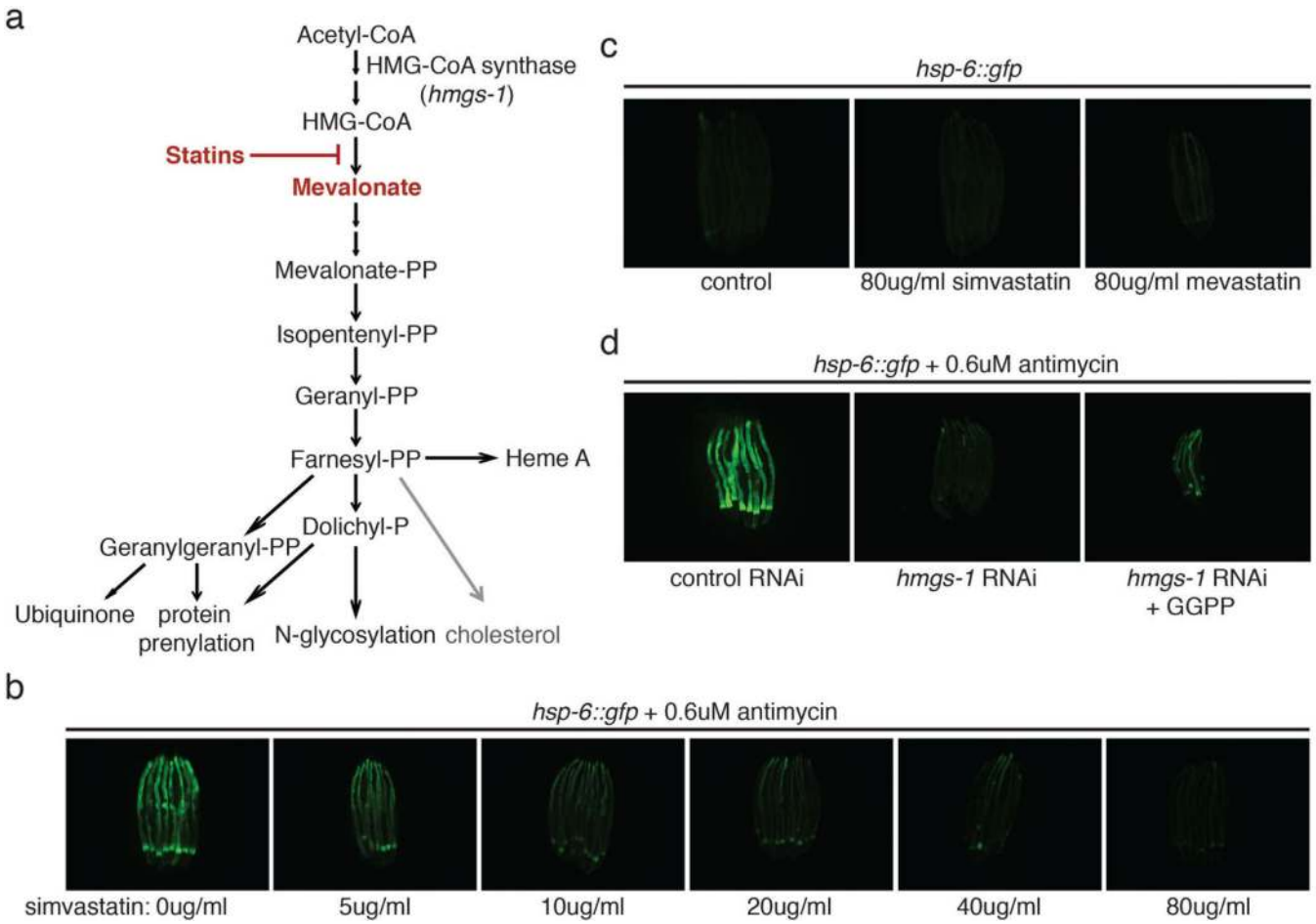

Extended Data Figure 8.

a, Diagram of the mevalonate pathway for the biosynthesis of cholesterol, ubiquinone and heme A, and protein N-glycosylation and prenylation. **b,** *hsp-6p::gfp* animals treated with antimycin after pre-treatment with increasing concentration of simvastatin. **c,** *hsp-6p::gfp* animals with mock, 80ug/ml simvastatin or 80ug/ml mevastatin treatment. **d,** *hsp-6p::gfp* animals raised on control RNAi, *hmgs-1* RNAi, or *hmgs-1* RNAi with the addition of geranylgeranyl pyrophoshate. The animals were then treated with antimycin to induce mitochondrial damage. Statin toxicity has been proposed to be caused by the inhibition of Rab prenylation[24]. Geranylgeranyl pyrophosphate (GGPP), a precursor of protein prenylation rescued the statin side effect in cell culture[24]. GGPP also partially rescued the deficiency of mitochondrial surveillance and activated *hsp-6p::gfp* in antimycin-treated *hmgs-1*(RNAi) animals.

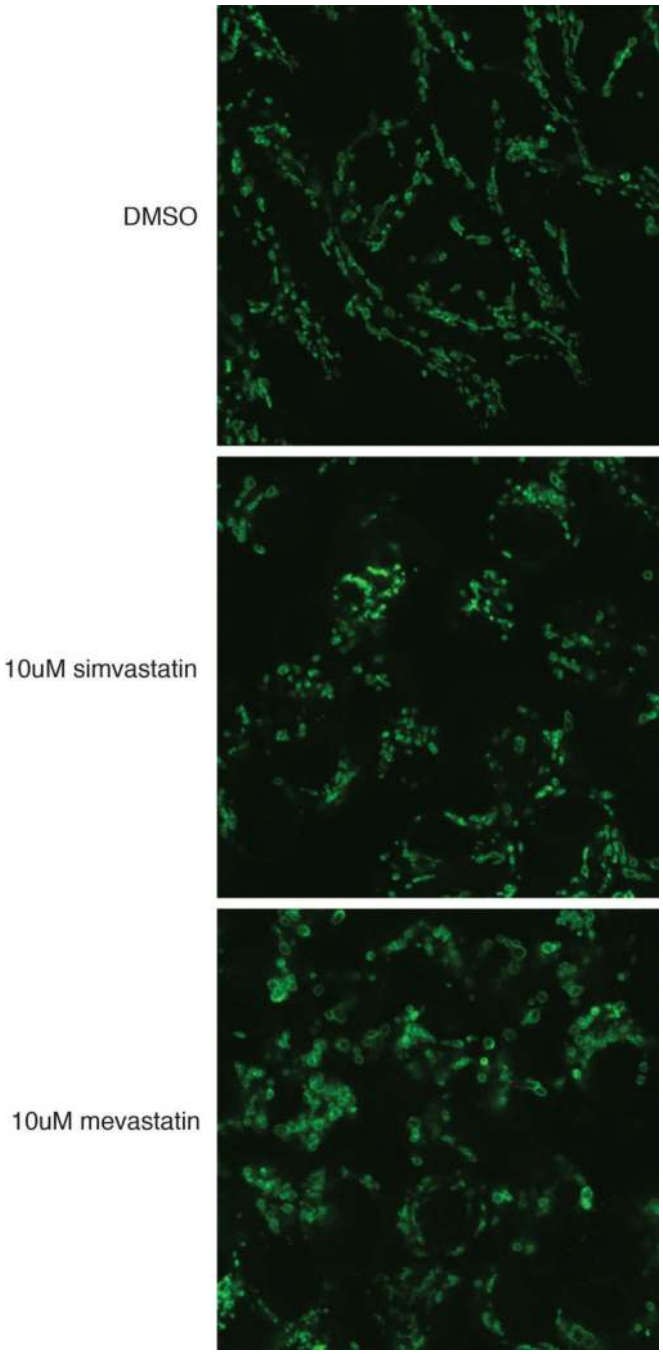

Extended Data Figure 9.

Mitochondrial immunostaining in HEK293T cells. The cells were treated with DMSO, 10uM simvastatin or 10uM mevastatin for 2 days.

Extended Data Table 1

Full list of genes identified in the genome-wide RNAi screen for mitochondrial surveillance. The table was sorted by the severity in the defect of the reporter gene induction. The intensity of blue denotes the severity of the defect in mitochondrial inactivation-induced gene response for each gene-inactivation, with darker blue showing the most severe failure to upregulate the response genes. Yellow color indicates previously reported genes for mitochondria unfolded response. N/A means the gene inactivations render the *isp-1; hsp-6::gfp* animals sick or lethal, which prevented assessment of GFP levels. The synthetic lethality of these mitochondrial surveillance defective gene inactivations with a

mitochondrial defect in *isp-1(qm150)* endorses their role in the homeostatic response that may allow the *isp-1(qm150)* mutant to be viable.

gene	*hsp-6p::gfp* +antimycin	*hsp-6p::gfp* on *atp-2*(RNAi)	*ugt-61p::gfp* +antimycin	*isp-1; hsp6::gfp*	Function
empty vector					
sptl-1					serine palmitoyl transferase
ran-4					nuclear transport
tag-214					E3 ubiquitin ligase
skp-1					transcriptional cofactor
npp-6					nuclear pore complex
Y47G6A.29					uncharacterized protein
let-70					E2 ubiquitin conjugating enzyme
thoc-2					transcription factor/nuclear export
syx-5				N/A	syntaxin, vesicular transport
snap-1				N/A	vesicular transport
gsp-2				N/A	Phosphatase
F40F12.7				N/A	CREB binding protein
atfs-1					transcription factor
W04A4.5					uncharacterized protein
imb-3					nuclear transport
smgl-1					SMG-associated and Lethal
hmgs-1					HMG-CoA synthase
Y54E10BR.5					signal peptidase complex subunit
F18F11.5					protein kinase
pas-3					proteasome subunit
nxt-1					nuclear export protein
clpp-1					mitochondrial protease
Y82E9BR.13					uncharacterized protein
fat-6					fatty acid desaturase
dve-1					DNA-binding protein
vps-32.2					vacuolar protein sorting
ast-1					transcription factors
wnk-1					protein kinase
unc-60					actin depolymerizing factor
inx-17					INneXin
pqn-92					glutamine/asparagine-rich
itr-1					inositol trisphosphate receptor
dss-1					26S proteasome subunit
M03F4.6					epidermal growth factor-like
sos-1					guanine nucleotide exchange
Y48G10A.4					uncharacterized protein
dcp-66				N/A	transcriptional repressor
hda-1					histone deacetylase 1
Y17G7B.18a					Methyltransferase
ceh-20					homeodomain co-factor
elo-3					fatty acid elongase
pkc-3					protein kinase
hpo-10					Hypersensitive to POre-forming toxin
ketn-1					transcription regulated by hypoxia
cdc-42					RHO GTPase

from the strongest inhibition to the weakest inhibition of GFP induction

N/A isp-1;hsp-6::gfp worms were lethal by the time to score

genes identified priviously to be involved in mitochondrial stress response

Supplementary Material

Refer to Web version on PubMed Central for supplementary material.

Acknowledgments

We thank Drs. C. Haynes (Memorial Sloan-Kettering Cancer Center), F. Ausubel (Massachusetts General Hospital), and the Caenorhabditis Genetics Center for providing strains; and V. Mootha lab (Massachusetts General Hospital) for providing the C2C12 cells. We thank J. Larkins-Ford, C. Phillips, S. Garcia, and M. Pellegrino for technical support, as well as MA. Félix for bacterial strains and for guidance in the collection of microbial strains from *C. elegans* natural habitats. Y.L. is supported by the Helen Hay Whitney research fellowship; B.S.S is supported by the Charles King Trust postdoctoral fellowship. The work is supported by a grant from the National Institute of Health awarded to G.R. (NIH AG043184-16).

References and notes

1. Melo JA, Ruvkun G. Inactivation of conserved C. elegans genes engages pathogen- and xenobiotic-associated defenses. Cell. 2012; 149:452–466. [PubMed: 22500807]
2. Runkel ED, Liu S, Baumeister R, Schulze E. Surveillance-activated defenses block the ROS-induced mitochondrial unfolded protein response. PLoS genetics. 2013; 9:e1003346. [PubMed: 23516373]
3. Benedetti C, Haynes CM, Yang Y, Harding HP, Ron D. Ubiquitin-like protein 5 positively regulates chaperone gene expression in the mitochondrial unfolded protein response. Genetics. 2006; 174:229–239. [PubMed: 16816413]
4. Haynes CM, Petrova K, Benedetti C, Yang Y, Ron D. ClpP mediates activation of a mitochondrial unfolded protein response in C. elegans. Developmental cell. 2007; 13:467–480. [PubMed: 17925224]
5. Haynes CM, Yang Y, Blais SP, Neubert TA, Ron D. The matrix peptide exporter HAF-1 signals a mitochondrial UPR by activating the transcription factor ZC376.7 in C. elegans. Molecular cell. 2010; 37:529–540. [PubMed: 20188671]
6. Nargund AM, Pellegrino MW, Fiorese CJ, Baker BM, Haynes CM. Mitochondrial import efficiency of ATFS-1 regulates mitochondrial UPR activation. Science. 2012; 337:587–590. [PubMed: 22700657]
7. Durieux J, Wolff S, Dillin A. The cell-non-autonomous nature of electron transport chainmediated longevity. Cell. 2011; 144:79–91. [PubMed: 21215371]
8. Pellegrino MW, Nargund AM, Haynes CM. Signaling the mitochondrial unfolded protein response. Biochimica et biophysica acta. 2013; 1833:410–416. [PubMed: 22445420]
9. Estes KA, Dunbar TL, Powell JR, Ausubel FM, Troemel ER. bZIP transcription factor zip-2 mediates an early response to Pseudomonas aeruginosa infection in Caenorhabditis elegans. Proceedings of the National Academy of Sciences of the United States of America. 2010; 107:2153–2158. [PubMed: 20133860]
10. Felix MA, Duveau F. Population dynamics and habitat sharing of natural populations of Caenorhabditis elegans and C. briggsae. BMC biology. 2012; 10:59. [PubMed: 22731941]
11. Lee SS, et al. A systematic RNAi screen identifies a critical role for mitochondria in C. elegans longevity. Nature genetics. 2003; 33:40–48. [PubMed: 12447374]
12. Menuz V, et al. Protection of C. elegans from anoxia by HYL-2 ceramide synthase. Science. 2009; 324:381–384. [PubMed: 19372430]
13. Deng X, et al. Ceramide biogenesis is required for radiation-induced apoptosis in the germ line of C. elegans. Science. 2008; 322:110–115. [PubMed: 18832646]
14. Sentelle RD, et al. Ceramide targets autophagosomes to mitochondria and induces lethal mitophagy. Nature chemical biology. 2012; 8:831–838.
15. Colombini M. Ceramide channels and their role in mitochondria-mediated apoptosis. Biochimica et biophysica acta. 2010; 1797:1239–1244. [PubMed: 20100454]
16. Wenner Moyer M. The search beyond statins. Nature medicine. 2010; 16:150–153.
17. Graham DJ, et al. Incidence of hospitalized rhabdomyolysis in patients treated with lipidlowering drugs. JAMA : the journal of the American Medical Association. 2004; 292:2585–2590. [PubMed: 15572716]
18. Rauthan M, Ranji P, Aguilera Pradenas N, Pitot C, Pilon M. The mitochondrial unfolded protein response activator ATFS-1 protects cells from inhibition of the mevalonate pathway. Proceedings

of the National Academy of Sciences of the United States of America. 2013; 110:5981–5986. [PubMed: 23530189]

19. Hage-Sleiman R, Esmerian MO, Kobeissy H, Dbaibo G. p53 and Ceramide as Collaborators in the Stress Response. International journal of molecular sciences. 2013; 14:4982–5012. [PubMed: 23455468]
20. Senkal CE, et al. Alteration of ceramide synthase 6/C16-ceramide induces activating transcription factor 6-mediated endoplasmic reticulum (ER) stress and apoptosis via perturbation of cellular Ca2+ and ER/Golgi membrane network. The Journal of biological chemistry. 2011; 286:42446–42458. [PubMed: 22013072]
21. Breslow DK, Weissman JS. Membranes in balance: mechanisms of sphingolipid homeostasis. Molecular cell. 2010; 40:267–279. [PubMed: 20965421]
22. Bookout AL, Mangelsdorf DJ. Quantitative real-time PCR protocol for analysis of nuclear receptor signaling pathways. Nuclear receptor signaling. 2003; 1:e012. [PubMed: 16604184]
23. Phillips CM, McDonald KL, Dernburg AF. Cytological analysis of meiosis in Caenorhabditis elegans. Methods in molecular biology. 2009; 558:171–195. [PubMed: 19685325]
24. Wagner BK, et al. A small-molecule screening strategy to identify suppressors of statin myopathy. ACS chemical biology. 2011; 6:900–904. [PubMed: 21732624]

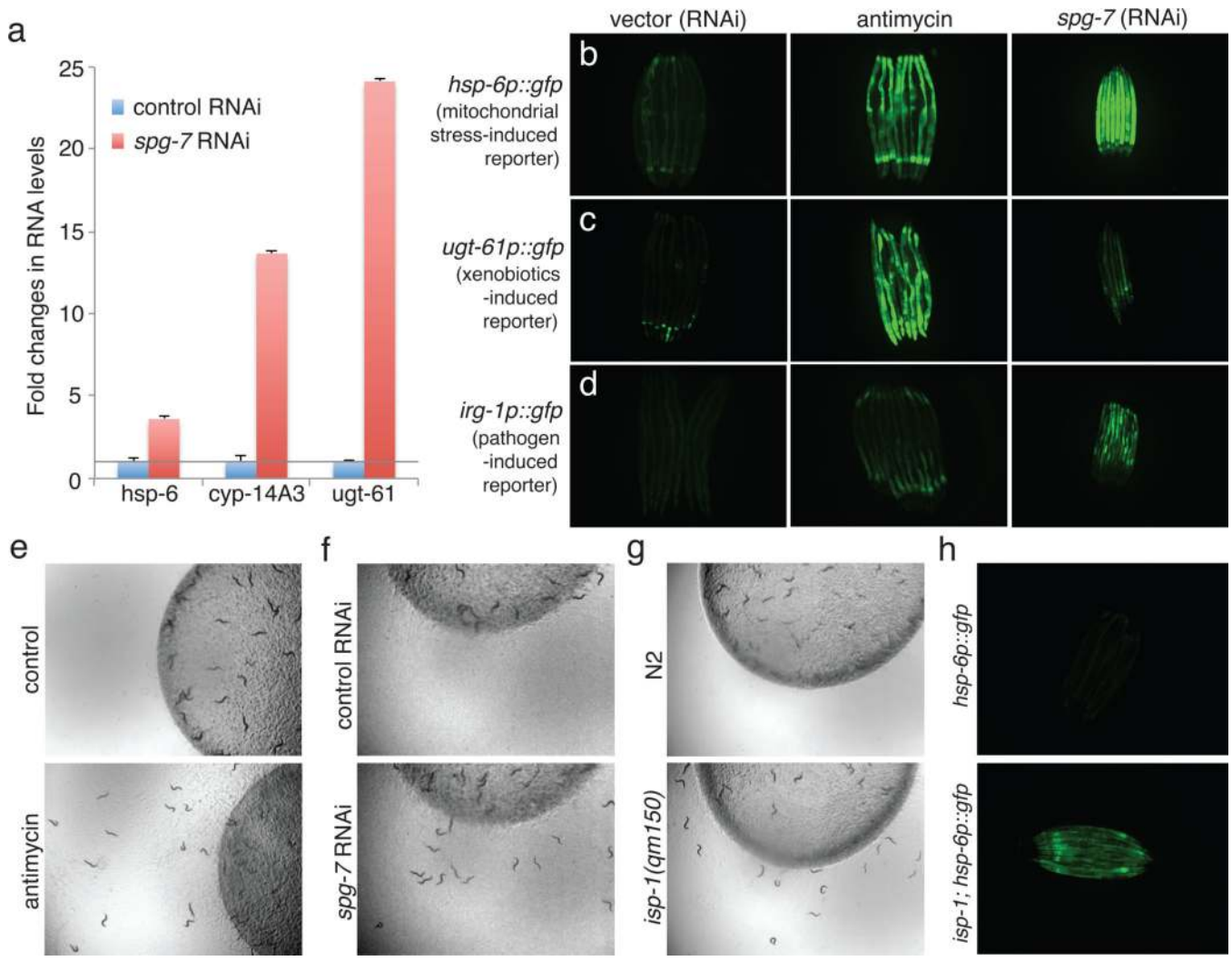

Figure 1.

Mitochondrial dysfunction activates homeostatic, detoxification and pathogen responses. **a,** mitochondrial chaperone and detoxification transcripts in control vs. *spg-7*(RNAi) (n=3). Error bars represent s.d. **b-d,** *hsp-6p::gfp* (b), *ugt-61p::gfp* (c), and *irg-1p::gfp* (d) animals raised on control *E. coli*, or *E. coli* with antimycin or *spg-7* (RNAi). **e-g,** Drug-, RNAi- or mutant allele-based mitochondrial inhibition causes food avoidance. **h,** wild type *hsp-6p::gfp* and *isp-1(qm150); hsp-6p::gfp* animals.

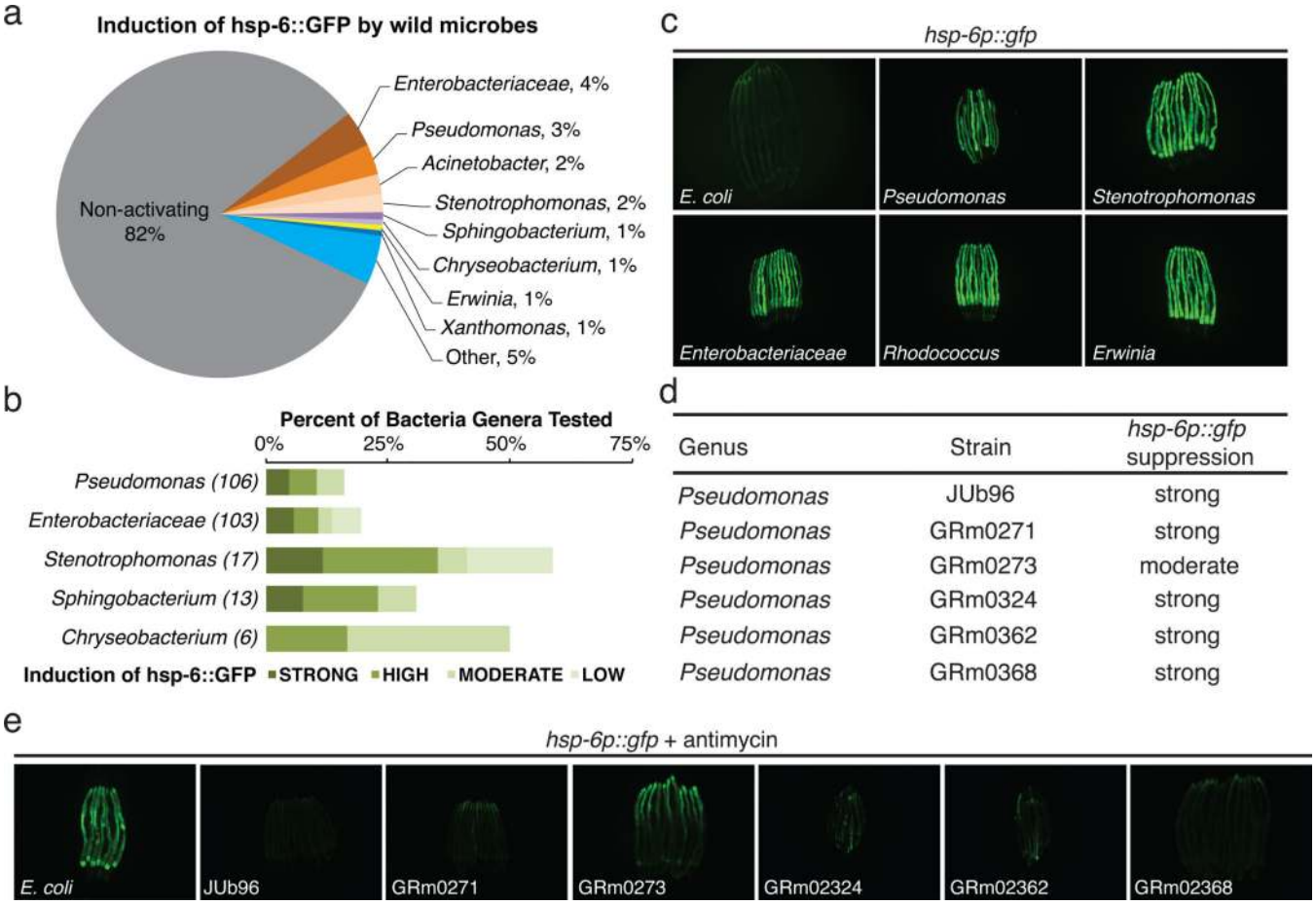

Figure 2.

Some bacteria from the *C. elegans* natural habitat antagonize the mitochondria. **a,** Genera that induce *hsp-6p::gfp* [100 of 560 tested microbes (18%)]. **b,** Proportion of bacterial genera tested that cause mitochondrial dysfunction and *hsp-6p::gfp* induction. **c,** *hsp-6p::gfp* animals raised on *E. coli* or natural microbial species. **d,** Six bacterial strains that render *C. elegans* defective in *hsp-6* response to antimycin. **e,** *hsp-6p::gfp* animals exposed to antimycin and raised on control *E. coli* or the six microbial strains.

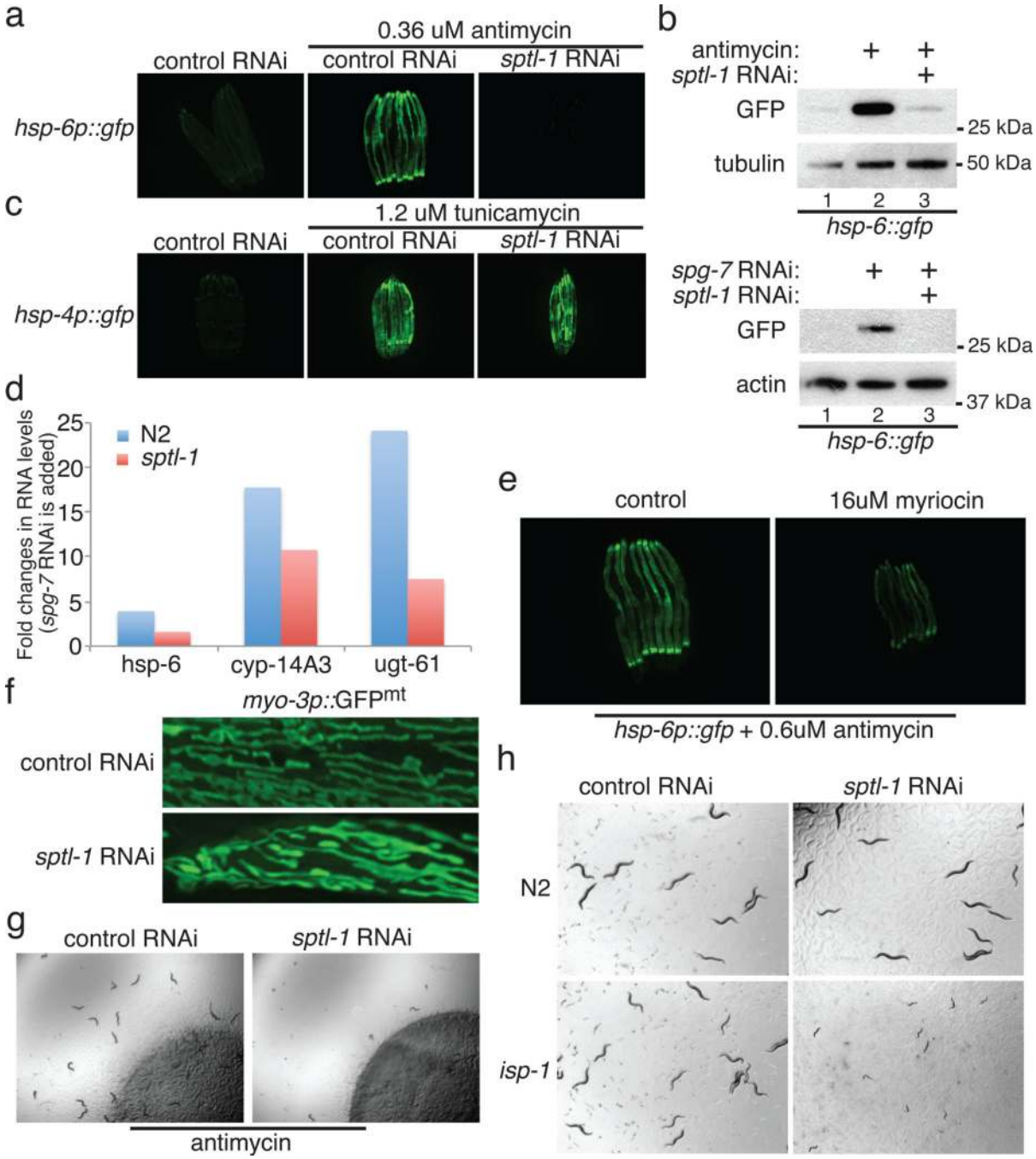

Figure 3.

The serine palmitoyl transferase *sptl-1* is required for mitochondrial surveillance. **a,** *hsp-6p::gfp* animals raised on control or *sptl-1*(RNAi) in the presence or absence of antimycin. **b,** GFP immunoblot expressed by *hsp-6p::gfp* animals in the presence or absence of antimycin or *spg-7*(RNAi). **c,** *hsp-4p::gfp* animals raised on control or *sptl-1*(RNAi) in the presence or absence of the ER drug tunicamycin. **d,** *C. elegans hsp-6* and xenobiotic detoxification gene transcripts in control or *sptl-1(ok1693)* mutant animals after exposure to *spg-7*(RNAi) (n=2). **e,** *hsp-6p::gfp* animals raised in the presence or absence of myriocin. **f,**

Body wall muscle of *sptl-1(RNAi)* compared to wild type animals expressing a mitochondrially localized GFP reporter. **g,** Food avoidance phenotypes for control or *sptl-1*(RNAi) animals treated with antimycin. **h,** Wild type or *isp-1(qm150)* raised on control or *sptl-1*(RNAi).

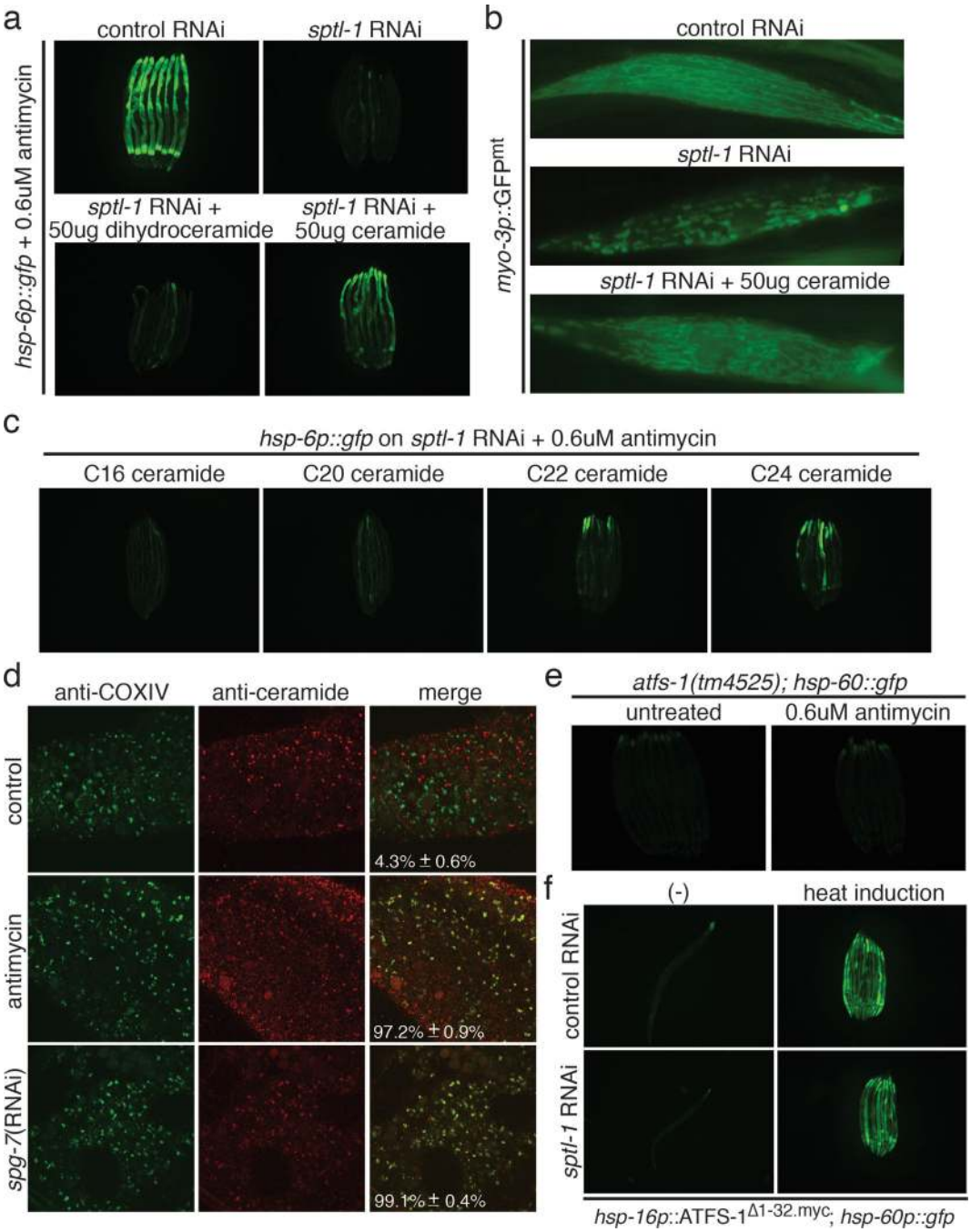

Figure 4.

Ceramide biogenesis is required for mitochondrial surveillance. **a,** *hsp-6p::gfp* animals exposed to antimycin in the presence or absence of dihydroceramide or ceramide. **b,** Body wall muscle of animals expressing a mitochondrially localized GFP reporter in *sptl-1*(RNAi) with and without added ceramide. **c,** *hsp-6p::gfp sptl-1*(RNAi) plus antimycin with different ceramide species. **d,** Dissected animals after antimycin or *spg-7*(RNAi) treatment were stained with anti-COX-IV (red) and anti-ceramide antibodies (green). Quantification represents proportion of mitochondria with contact of mitochondrial and ceramide staining

(mean ± s.d., n=3). **e,** *atfs-1(tm4525); hsp-60p::gfp* animals alone or with antimycin. **f,** *atfs-1(tm4525)*; *hsp-16p::*ATFS-1$^{\Delta 1\text{-}32.myc}$; *hsp-60p::gfp* animals raised on control or *sptl-1*(RNAi).